

**SIXTH EUROPEAN ROTORCRAFT AND POWERED LIFT AIRCRAFT FORUM**

Paper No. 26

**AERODYNAMIC STUDY OF A HOVERING ROTOR**

by

**J.M. POURADIER**

Société Nationale Industrielle Aérospatiale

Helicopter Division  
Marignane, France

and

**E. HOROWITZ**

O.N.E.R.A.

September 16 -19, 1980

Bristol, England

**THE UNIVERSITY, BRISTOL, BS8 1HR, ENGLAND**

# AERODYNAMIC STUDY OF A HOVERING ROTOR

E. HOROWITZ (O.N.E.R.A.) and J.M. POURADIER (S.N.I.A.)

## SYMBOLS USED

b	: number of blades on rotor
c	: blade chord (m.)
e	: absolute thickness of blade profile (m.)
R	: rotor radius (m.)
r, z, $\Psi$	: ordinates of any point in a system of cylindrical coordinates in which the z axis is the rotor axis and the r axis is the span axis of one blade chosen as the reference blade (r and z are in m., $\Psi$ is in $^\circ$ )
x	: chordwise position of a blade point
$C_T/\sigma$	: $\frac{Fz}{\rho b c R u^2}$
Fz	: rotor lift (N)
$\rho$	: air density ( $\text{kg/m}^3$ )
u	: circumferential velocity (m/sec)
$V_T$	: tangential velocity (m/sec)
$V_z$	: axial velocity (m/sec)
$V_{Sj}(r)$	: axial speed induced at the r axis point on blade 1 by the vortex sheet $S_j$ from blade j (m/sec)
$V_{Vj}(r)$	: axial speed induced at the r axis point on blade 1 by the tip vortex $V_j$ from blade j (m/sec)

## 1 – INTRODUCTION

ONERA and Aerospatiale have started a joint research programme aimed at improving helicopter rotor performance. The main lines of this programme are as follows :

- further study of the airflow at the blade tip,
- development of methods for calculating this airflow,
- improvement and validation of methods for calculating rotor performance.

Research on hovering flight is a major part of the programme. This paper summarizes the results obtained to date on hovering flight. In reference 1, Mr J.J. Philippe and Mr. J.J. Chattot will report on research directed more particularly to forward flight.

In the first section we will describe the test facilities used and analyse the results of wind-tunnel testing on a 3-bladed rotor.

In the second section, we will be describing a programme of performance calculation for rotors in hover based on the vortex theory. This programme provides for partial free

wake analysis. We will then compare the theoretical and the experimental results in order to establish the possible improvements.

## 2 – EXPERIMENTAL RESEARCH\*

This research is aimed at improving our knowledge of the aerodynamic behaviour of the blade tips and at establishing the data required for the development and validation of the methods of calculation. It involves wind-tunnel experiments on a 3-bladed rotor.

### 2.1 – Test facilities

The Chalais-Meudon S2 wind-tunnel has a 3 m diameter test section. For the hovering flight tests, the side walls and roof of the vein are removed to limit the wall effects (the rotor lift is directed downwards). Fig. 1 shows the installation of the rotor and the laser velocimeter in the vein.

The main characteristics of the rotor are these :

- flapping, lag and pitch hinges,
- number of blades : 3,
- rotor radius : 0.857 m,
- chord : 0.123 m,
- blade profiles Aerospatiale SA 13112 ( $e/c = 12\%$ ) up to 0.7 R  
Aerospatiale SA 13109 ( $e/c = 9\%$ ) at 0.9 R  
Aerospatiale SA 13106 ( $e/c = 6\%$ ) at R.
- linear twist —  $12.1^\circ$  (theoretical twist)

The blade tips are removable at 0.78R. For these tests the tips were rectangular.

The tips were fitted with 36 Kulite LDQL absolute pressure sensors in 3 sections located at 0.85 R, 0.90 R and 0.95 R. Each sensor is connected by a T-shaped tube to the upper and lower blade surfaces, so that by blocking off the upper or lower pressure inlets, it is possible to obtain 72 absolute pressure measurements per configuration.

\*This research was carried out with financial support from the Service Technique des Programmes Aéronautiques of the French Ministry of Defence.

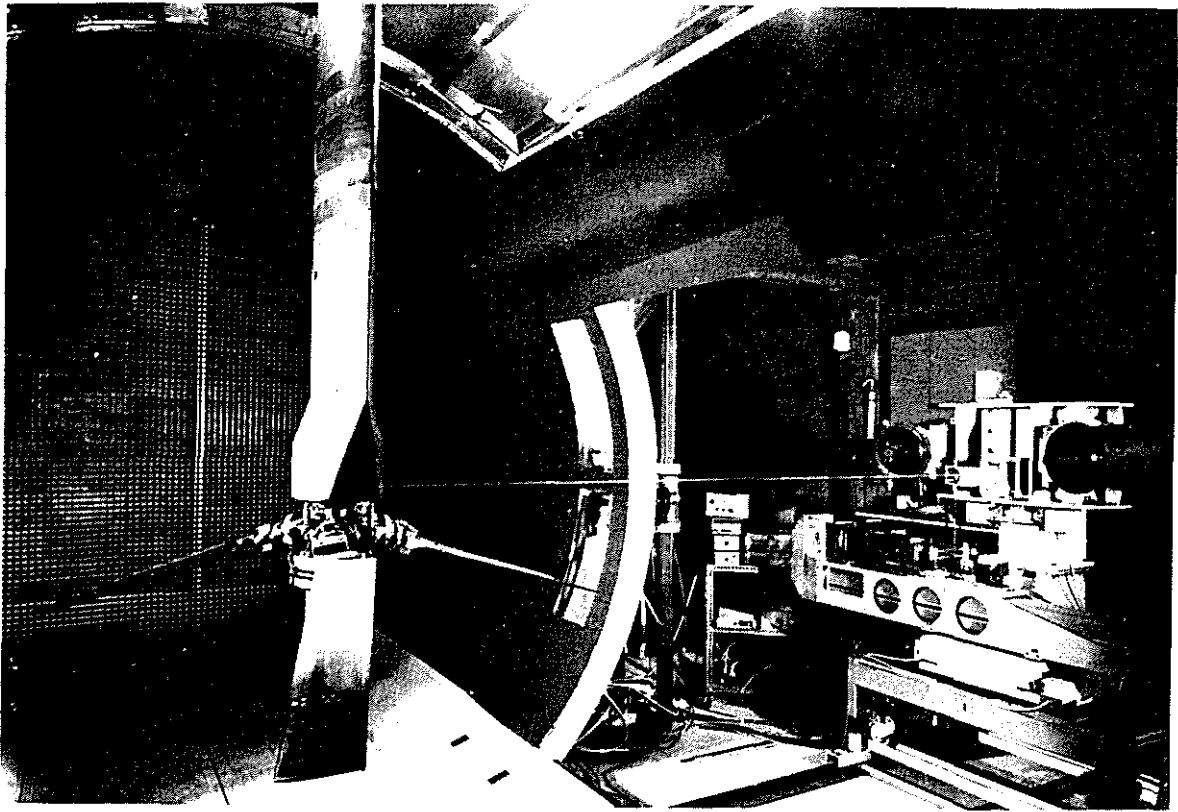


Figure 1 : LASER VELOCIMETER AND 3-BLADED ROTOR IN S2 CH WIND TUNNEL

The induced velocities are measured using a 2-component laser velocimeter developed by ONERA. Its arrangement is given in fig. 2. This velocimeter works by retrodiffusion of light and uses the classical technique of interference fringes. It is fitted with Bragg cells, which serve to determine the velocity sign.

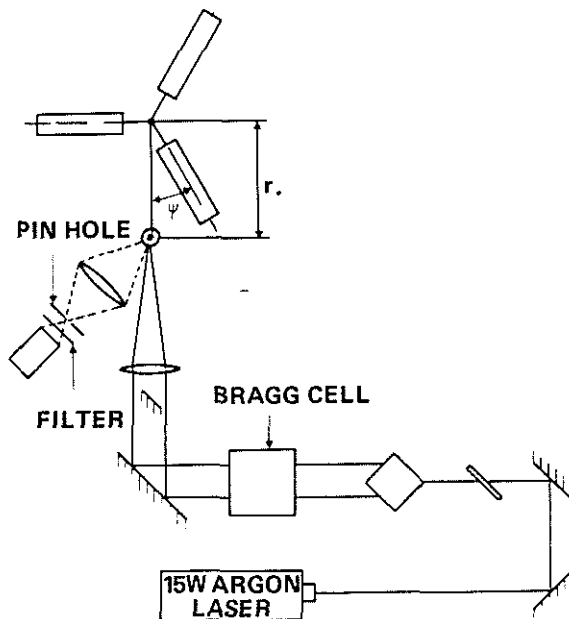


Figure 2 : OPTICAL ARRANGEMENT OF LASER DOPPLER VELOCIMETER

Azimuth can be ascertained at all times by a system of toothed wheels. A few tests are conducted with a level detector and a logical validation unit, in order to eliminate signals due to noise or to excessively large particles. If validated, the signal and the corresponding azimuth are sent to a computer which then determines the average velocity and standard deviation at each azimuth for a pre-established number of samples. Fig. 3 is a flow diagram of the data acquisition and processing unit. The maximum data acquisition speed is 100,000 samples per second and the maximum measurable frequency is 100 MHz.

## 2.2 — Test programme

Since a hovering rotor's performance is affected mainly by that part of the tip vortex path which is close to the rotor (cf. § 3.2), the test programme was designed to enable this part of the path to be established as accurately as possible.

The induced velocity measurement area and the various conventional symbols and notations are given in fig. 4. The measurement points and blade tip vortex path are shown by means of a system of cylindrical ordinates  $r, \Psi, z$  in which the  $z$  axis is the rotor axis and the  $r$  axis is the span axis of one blade used as a reference blade. In the case of tip vortex, the reference blade is the one from which the vortex originates. The measurement planes were chosen so that they would be crossed by the tip vortices in  $\Psi$  azimuths of  $60^\circ, 90^\circ, 120^\circ, 150^\circ$  and  $180^\circ$ , according to the tip vortex path modelling formulae given in reference 2. These planes go by stages from  $0.0257 R$  to  $0.165 R$

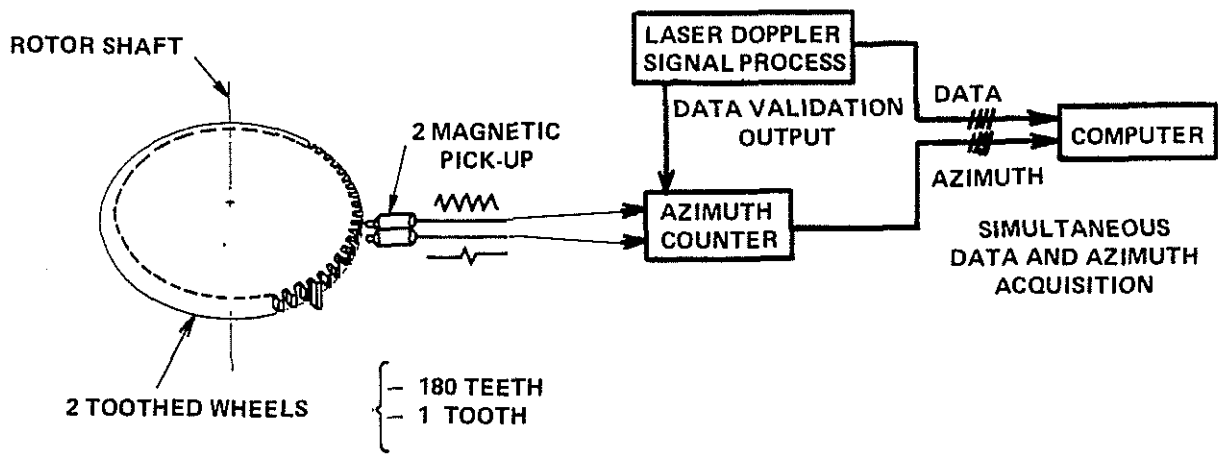


Figure 3: AZIMUTHAL LOCATING

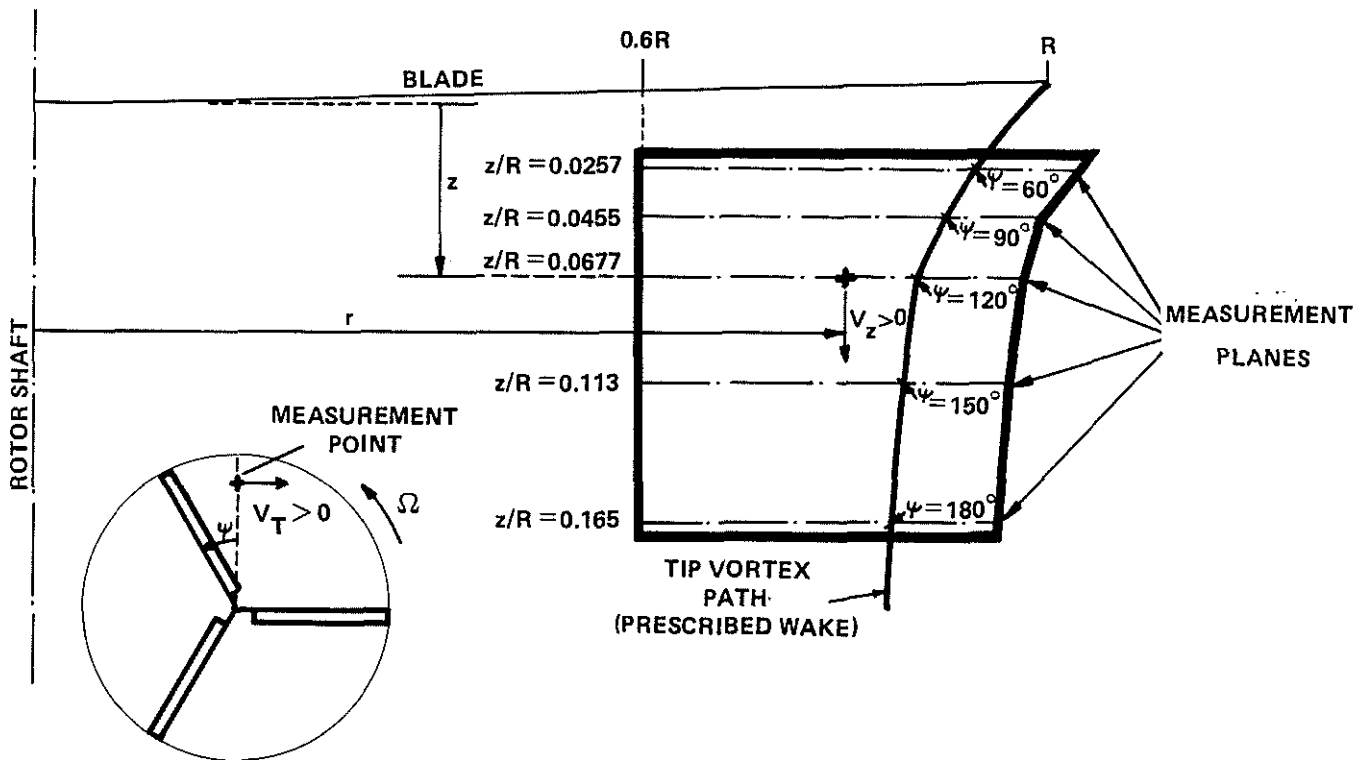


Figure 4: MEASUREMENT AREA

downstream from the hub plane. The plane corresponding to  $\Psi = 120^\circ$  ( $z/R = 0.0677$ ) is of particular interest because it is located at the theoretical level of the tip vortex as it first interacts with a blade. Radially, the measurement area goes from  $0.6 R$  to about  $0.1 R$  beyond the tip vortex's theoretical path.

These tests were conducted with a circumferential velocity of  $210 \text{ m/sec}$  and a  $C_T/\sigma$  of  $0.075$ .

### 2.3 – Experimental results

Some typical results are given in fig. 5, which shows the development in time of vertical induced velocities at 4 points on the same horizontal plane. This enables us to distinguish three main areas :

– At point M the vertical induced velocity is positive

and high in value (within the general range of momentum theory velocity) and it is practically constant in time. We will say that point M is located inside the wake.

– The tip vortex passes close to points N and N', causing large and rapid variations in the vertical induced velocities at these points. The direction of these variations is directly linked to the position of the measurement point relative to the tip vortex path.

– At point P the vertical induced velocity is negative, low in value and practically constant in time. When point P moves away from the rotor axis its vertical velocity tends rapidly towards zero. We will say that point P is located outside the wake.

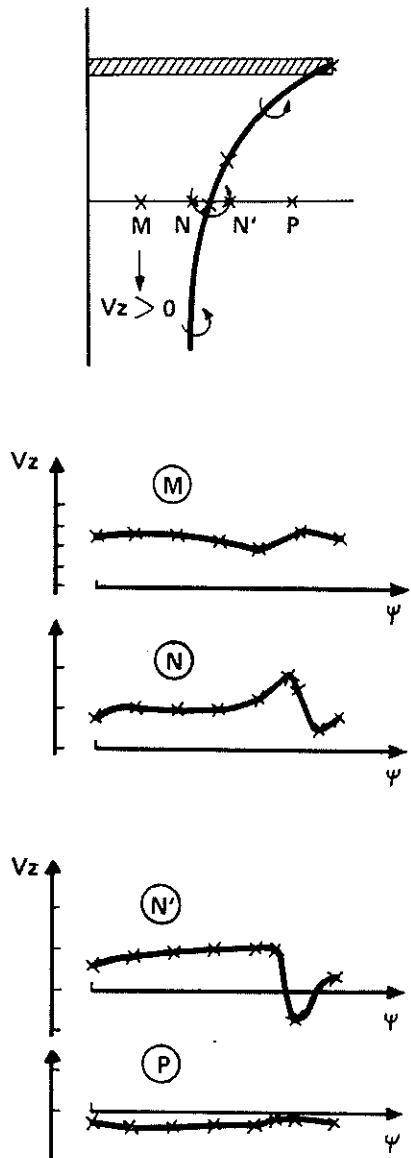


Figure 5 : AZIMUTHAL EVOLUTION OF AXIAL INDUCED VELOCITIES UNDER THE ROTOR DISC

Fig. 6 shows the variation with azimuth of the vertical induced velocities measured on the plane  $z/R = 0.0677$  for various radii. It can be seen that the tip vortex passes this measurement plane when the azimuth is roughly  $130^\circ$ , and not  $120^\circ$  as would be expected from applying the modelling formulae given in reference 2.

Using these measurements we can plot the radial distribution of the vertical induced velocities for various azimuths (fig. 7). These distribution patterns reveal another important characteristic of the inside of the wake : in this area, the axial velocities depend very little on the radius. At the edge of the wake there are jumps in velocity the size of which is related to the nearness of the tip vortex. The graphs for  $\Psi = 128^\circ, 130^\circ, 132^\circ$  and  $134^\circ$  can be used to plot the intersection of the tip vortex and this measurement plane at  $\Psi = 132^\circ$  and  $r = 0.85 R$ .

(EXPERIMENT -  $z/R = 0.0677 \cdot C_T / \sigma = 0.075$ )

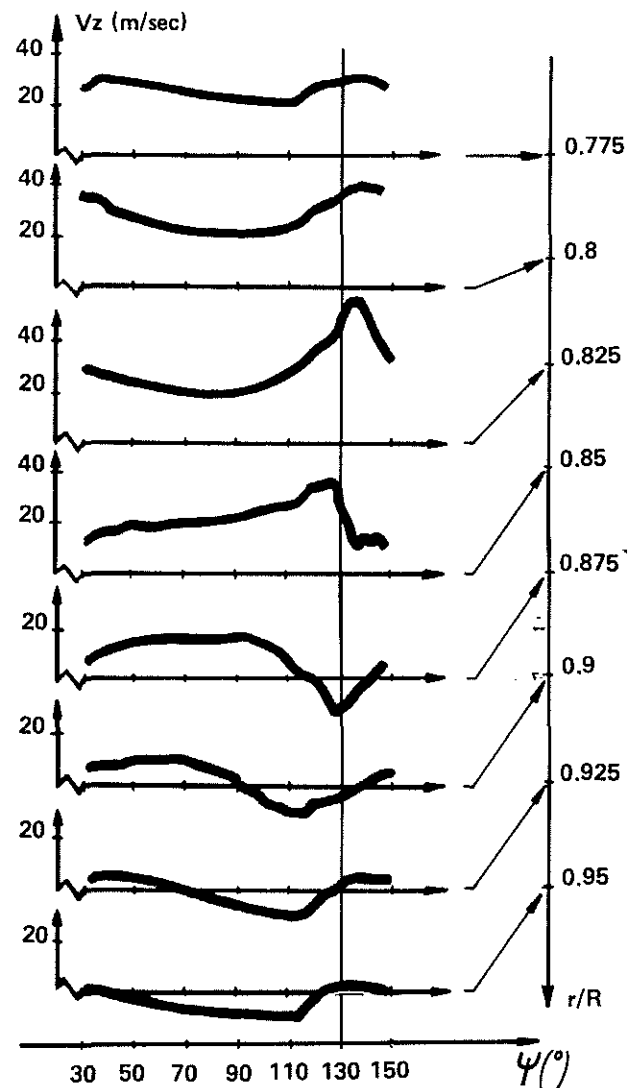
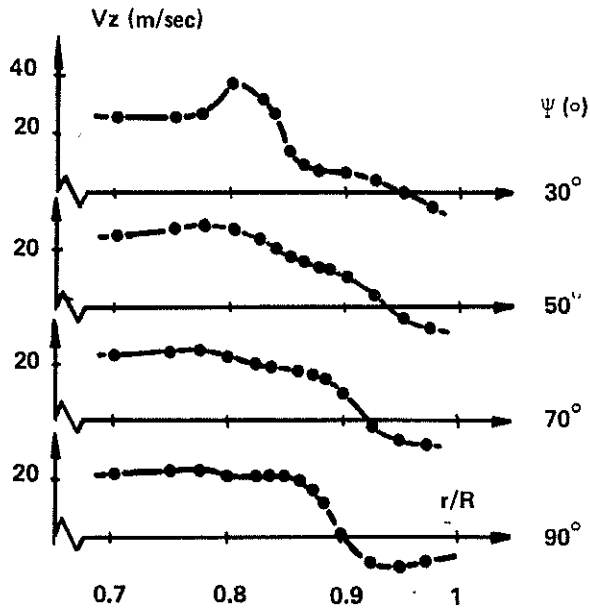


Figure 6 : AZIMUTHAL DISTRIBUTION OF VERTICAL INDUCED VELOCITIES

By repeating these measurements at different levels downstream from the rotor disk, the laws governing the descent and contraction of the tip vortex can be established and thus its path (fig. 8). Focussing our attention on the wake edge, we can also study in detail the tip vortex core structure and its development.

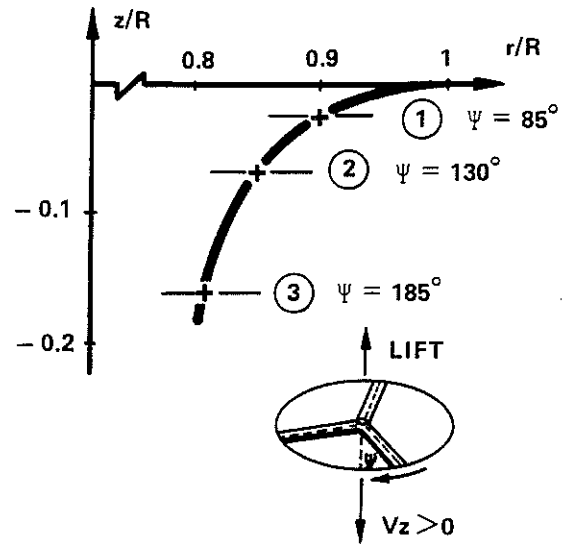
The tip vortex path was determined in two vertical planes, one containing the longitudinal axis of the airflow vein and the other the transverse axis.

(EXPERIMENT -  $z/R = 0.0677 \cdot C_T / \sigma = 0.075$ )



(EXPERIMENT -  $C_T / \sigma = 0.075$ )

TIP VORTEX TRAJECTORY



RADIAL DISTRIBUTION OF THE VERTICAL COMPONENT OF THE INDUCED VELOCITY.

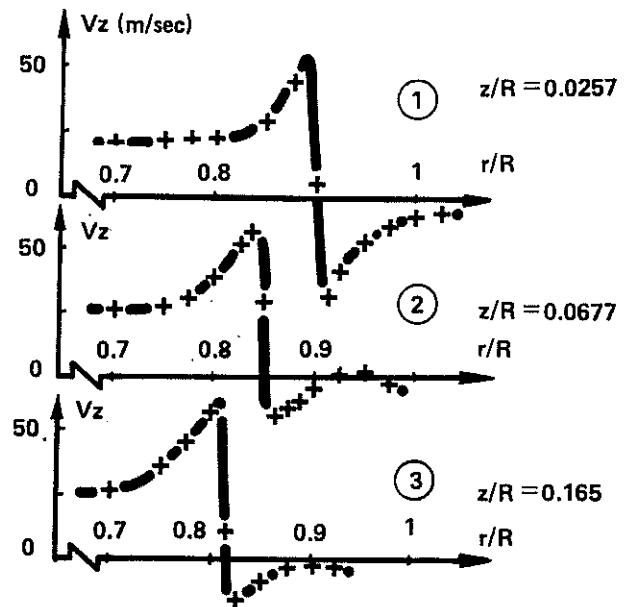
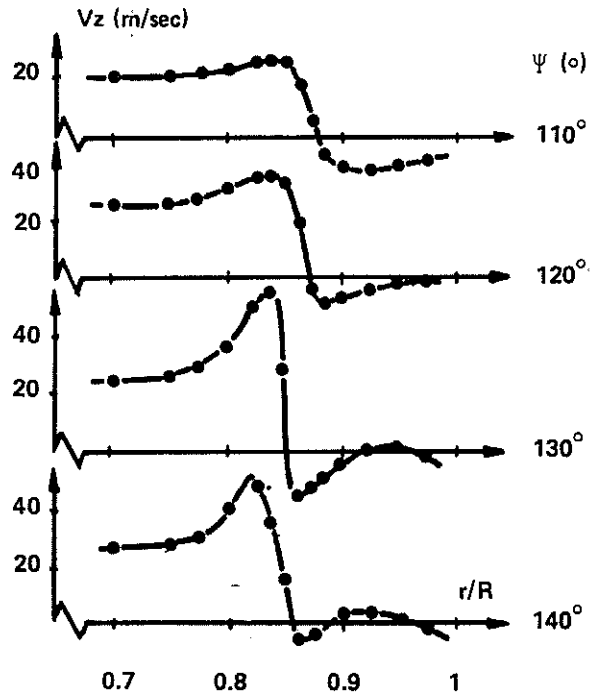


Figure 7: RADIAL DISTRIBUTION OF VERTICAL INDUCED VELOCITIES

Figure 8: TIP VORTEX PATH DETERMINATION

The paths observed in the two planes are appreciably different ; the vortex observed along the transverse axis descends slightly more quickly and its path is more contracted (fig. 9). Also, this vortex is less diluted than the other (fig. 10). In order to understand these differences, we have studied the changes in time of the instantaneous

pressures on the blade tip. The pressure changes at  $x/c = 0.1$  are shown in fig. 11 for 3 sections,  $r/R = 0.85, 0.9$  and  $0.95$ . It is seen that the  $K_p$  does not remain constant over a complete turn of the rotor ; there is one azimuth sector in which the  $K_p$  varies little (around  $\Psi = 270^\circ$ , i.e. around the transverse axis) and one azimuth sector

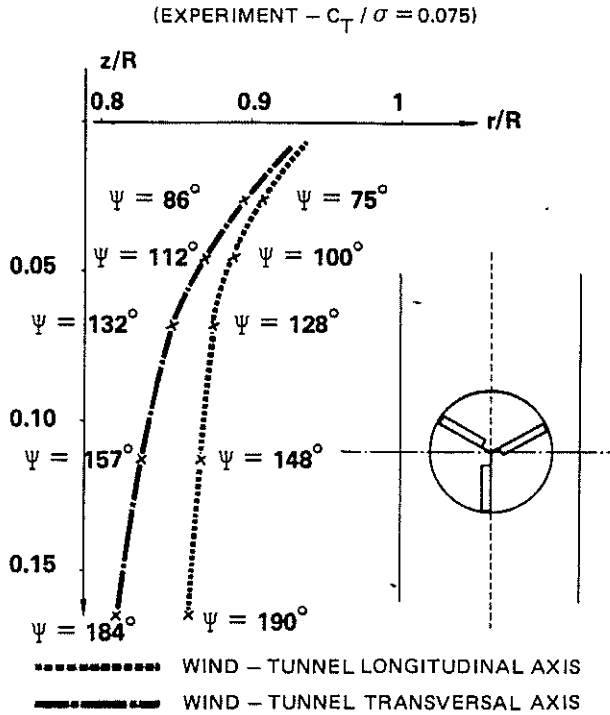


Figure 9 : COMPARISON OF TIP VORTEX PATHS MEASURED ON WIND TUNNEL LONGITUDINAL AND TRANSVERSAL AXIS

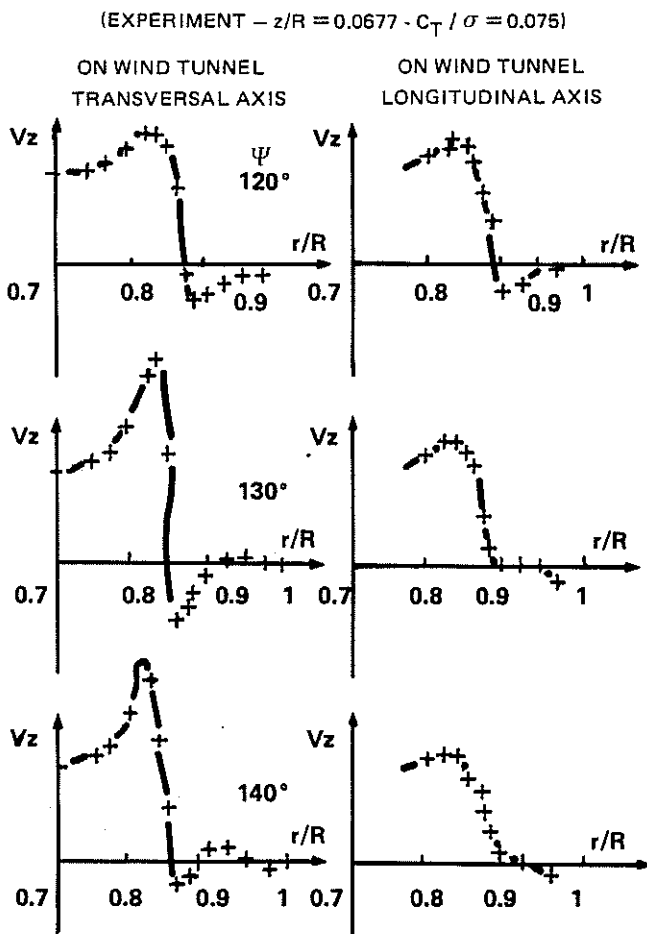


Figure 10 : RADIAL DISTRIBUTION OF VERTICAL INDUCED VELOCITIES

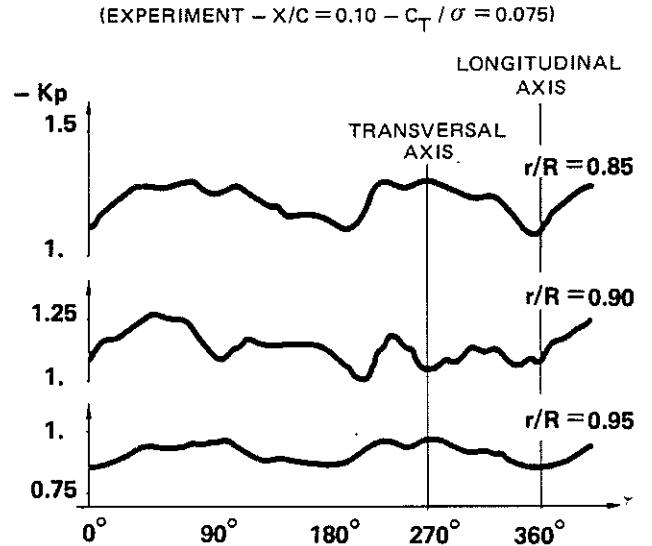


Figure 11 : AZIMUTHAL EVOLUTION OF PRESSURE ON THE BLADES

where it varies a lot (around  $\Psi = 0^\circ$ , i.e. around the longitudinal axis). These fluctuations in pressure, probably due to some effects of the few residual walls are the likely cause of the path differences. Research is underway at the ONERA hydraulics tank to attempt to define the origin of these fluctuations and to find possible remedies. Because of the relative constancy of pressures on the blade around the transverse axis we will only give below the results taken on that axis. This applies to the tangential induced velocities which we are about to discuss.

Qualitatively, the time and radial distributions of tangential induced velocities are the same in all the measurement planes. Since they are more characteristic near the rotor disk, we have shown on figs. 12 and 13 those measured in the plane of  $z/R = 0.0257$ . In one given point we observe up to 3 tangential velocity peaks.

- The first peak occurs when the tip vortex passes close to the measurement plane. It is clearly located in time and space ( $\Psi \cong 85^\circ$  and  $r/R = 0.9$  for this measurement plane).
- The second peak is observed around  $120^\circ$ , whatever the radial ( $r/R$ ) and axial ( $z/R$ ) position of the measurement point. It coincides with the blade's passage over the measurement point.
- The third peak is observed, for this measurement plane, at about  $\Psi = 140^\circ$ , and it is appreciable at  $0.8 \leq r/R \leq 0.95$ . Its cause is hard to establish, but it may be due to the start of rolling in the vortex sheet.

Apart from these peaks, the tangential velocities are low (4 or 5 times lower than the axial velocities) and generally in the direction of the blade's rotation.

This research demonstrates the usefulness of the laser velocimeter for studying the aerodynamic functioning of a hovering rotor. It can be used to study the wake geometry and the formation and dilution of the various vortex

elements. This data can in turn serve to refine the wake modelling required in performance calculation programmes for hovering rotors.

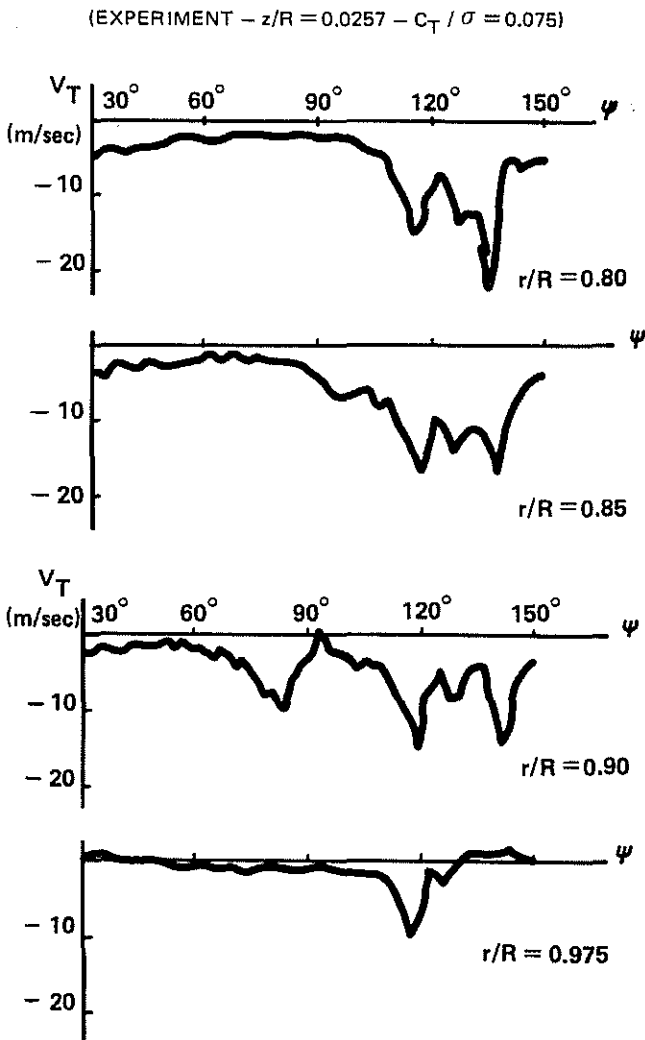


Figure 12 : AZIMUTHAL EVOLUTION OF TANGENTIAL INDUCED VELOCITIES

(EXPERIMENT -  $z/R = 0.0257 - C_T / \sigma = 0.075$ )

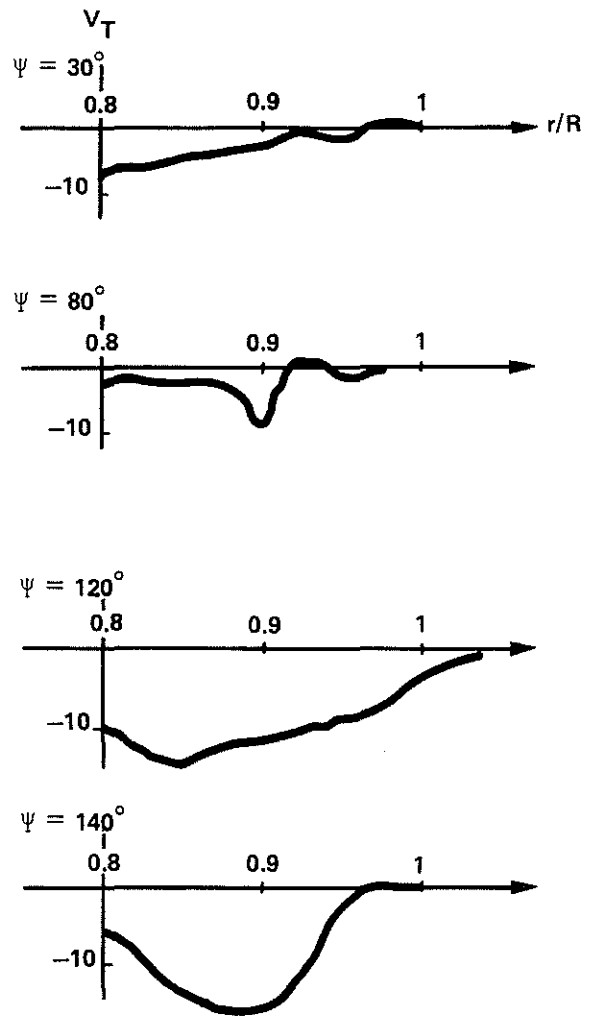


Figure 13 : RADIAL DISTRIBUTION OF TANGENTIAL INDUCED VELOCITIES

### 3 - THEORETICAL RESEARCH\*

#### 3.1 - Prescribed wake calculation programme

In 1975, Aérospatiale started a performance calculation programme for rotors in hover using the vortex method.

The main calculation assumptions are the following :

- the blade is rigid and has only a flapping hinge. It is represented by a lifting line,
- the circulation distribution is continuous on the blade and on the vortex sheet,
- the aerodynamic characteristics of the airfoils result from two-dimensional steady tests, so that it is possible to allow for non-linear aerodynamic phenomena and for compressibility effects.

For the first version the wake geometry was pre-set. It was calculated using the modelling formulae given in references 2 and 3. In particular, the description of the recirculation mechanism proposed in ref. 2 was adopted ; the recirculation resulting from the interactions between the tip vortices is represented by a vortex ring centred on the rotor axis, with the same radius as the rotor, located at the level of the 4th passage of the tip vortex beneath a blade and with an intensity 4 times that of the tip vortex. Fig. 14 shows the resulting representation of the wake. This schematized wake will be referred to as a «prescribed wake».

\*This research was financed by the French Min. of Defence Direction des Recherches Etudes et Techniques (Research, Design and Technology Dept.).

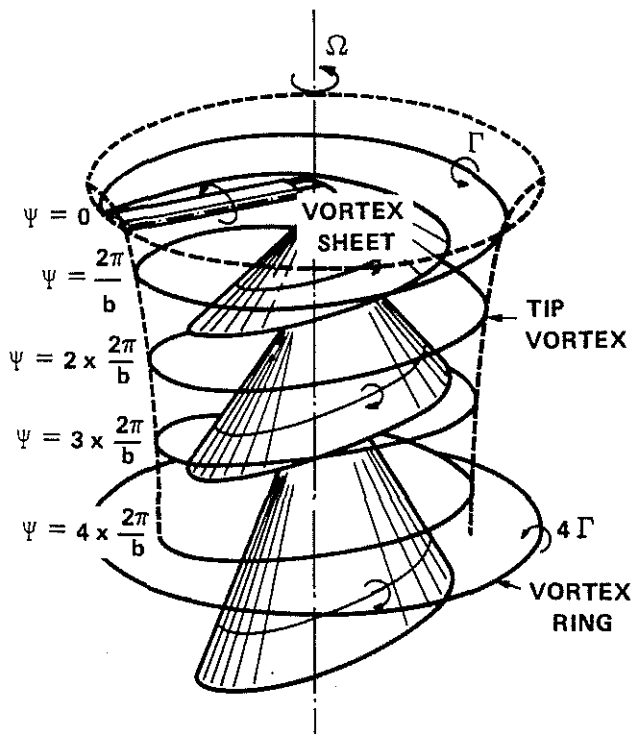


Figure 14 : SCHEMATIC OF ROTOR WAKE STRUCTURE

### 3.2 - Free wake analysis

The applicability of the schematized prescribed wake is relatively limited (e.g. : linear twist, moderate rotor load...)

and this limits the applications of the first version of the programme. Aerospatiale therefore started research in 1977 into free wake analysis.

It swiftly became apparent that free wake analysis for the whole of the close wake would lead to a prohibitive development period for the programme and also to a programme requiring a very large amount of CPU computing time. In order to determine which parts of the wake should be analyzed to achieve the best compromise between adequate performance calculation and computing time, a comparative study was made of the influence of each of the wake elements on the velocities induced on the blade. This research was done on the 3-bladed rotor described in para. 2.1.

The wake consists of  $2b$  main elements ; the  $b$  vortex sheets and the  $b$  tip vortices. Let us designate the vertical velocities induced at the ordinate point  $r$  on blade 1, first by the blade  $j$  whole vortex sheet  $S_j$  and secondly by its tip vortex  $V_j$ , as respectively  $V_{S_j}(r)$  and  $V_{V_j}(r)$ . The graphs of the functions  $V_{S_j}(r)/V_{V_1}(R)$  and  $V_{V_j}(r)/V_{V_1}(R)$  are shown in figure 15 for a given calculation example ( $u = 210$  m/s,  $C_T/\sigma = 0.075$ , prescribed wake analysis). The highest incident velocities are found at the tip, and so we will concentrate on the induced velocities at the tip. We observe that the effects of the vortex sheets are small when compared to those of the tip vortices. The tip vortex from blade 1 itself has a great effect on the extreme blade tip ( $r/R \geq 0.9$ ) because of the

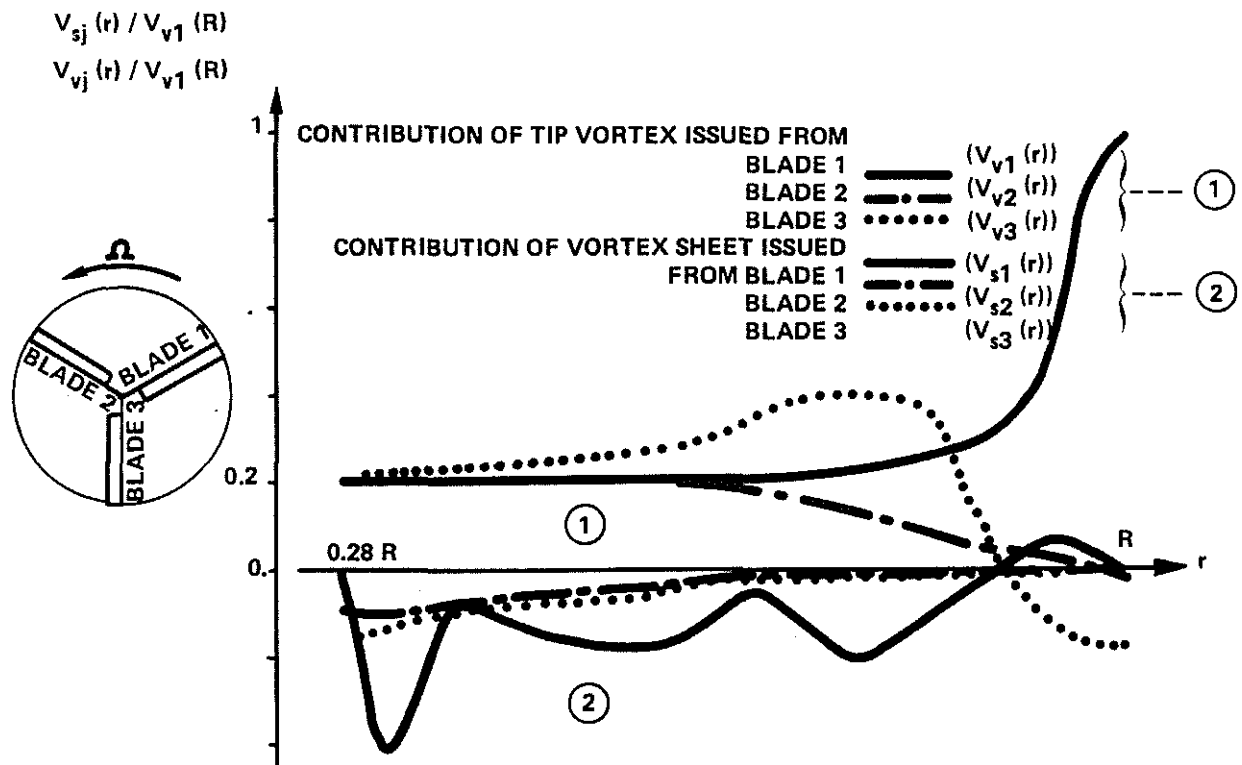


Figure 15 : CONTRIBUTIONS OF TIP VORTICES AND VORTEX SHEETS TO AXIAL INDUCED VELOCITIES ON BLADE 1

proximity of the blade tip vortex to the blade tip. The influence of the tip vortex from the preceding blade (blade 3) comes mainly from the first vortex interaction. The tip vortex from blade 2 has little effect. In view of the above, we decided on free wake analysis only for the tip vortices and then only between the moment they leave the trailing edge of the originating blade and the moment they pass beneath the next blade. Beyond that, their apparent axial and radial velocities are assumed to be equal to those given in reference 2.

Free wake analysis is achieved by the iterative process shown on the block diagram fig. 16. The initial wake geometry is that of the prescribed wake, and the initial circulation distribution on the blade is that which fits the prescribed wake geometry. The calculation stages are as follows :

1<sup>st</sup> stage : the circulation distribution on the blade being known, the induced velocities are calculated for each defining point on the tip vortex path.

2<sup>nd</sup> stage : the tip vortex path is changed so that it is tangent to the induced velocities calculated for each point.

Stages 1 and 2 are repeated until the vortex path is stabilized.

3<sup>rd</sup> stage : calculation of the circulation distribution on the blade that is compatible with the wake geometry obtained. At each repetition, the collective pitch is changed so as to maintain constant rotor lift.

Stages 1 to 3 are repeated until the circulation distribution on the blade is stabilized.

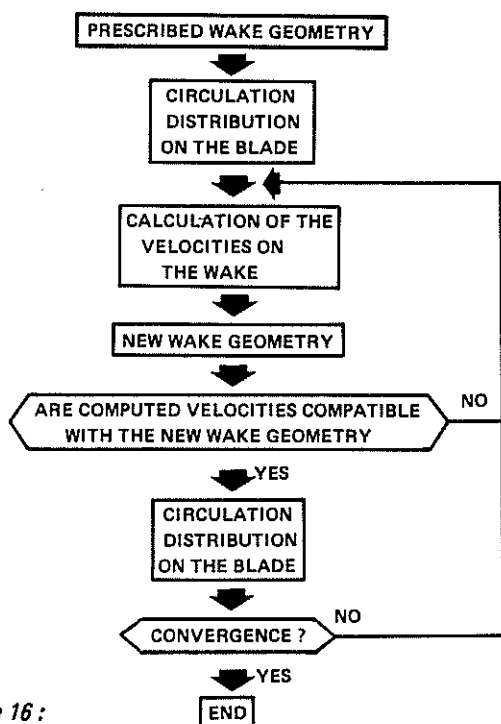


Figure 16 :

### 3.3 – Comparison between experiments and calculations

The first comparisons (on 3 or 4-bladed rotors) were not very satisfactory, and this caused us to modify the values of certain parameters of the vortex ring representing recirculation. The comparisons were much improved when the vortex ring radius was taken to be 1.2 times that of the rotor and when its intensity was taken to equal the product of the tip vortex intensity multiplied by the number of blades ; however, its level was still that of the 4<sup>th</sup> passage of the tip vortex beneath a blade. The comparisons given below were made using the new parameter values.

#### 3.3.1 – Comparison of calculated and experimental performance

Although partial, this free wake analysis led to a great improvement in performance calculation for a hovering rotor, while the computing time remained short enough to allow frequent and rapid use to be made of the programme. A complete calculation generally takes less than 20 CPU seconds on an IBM 3032.

The improvement of performance calculation by free wake analysis is illustrated by the following table, which compares the experimental and the calculated figure of merit of two rotors with different geometry.

Calculation example : 4-bladed rotor

rotor radius : 0.737 m  
 chord : 0.05 m  
 circumferential velocity : 196 m/s  
 rotor load :  $C_T/\sigma = 0.068$

Rotor	Experiment	Calculation	
		prescribed wake	free wake
Rectangular blades	0.645	0.653	0.645
tapered blades (taper of 0.5 over 0.05 R)	0.645	0.665	0.645
difference	0.000	+0.012	0.000

The comparisons between experiments and calculations are less good when the rotor approaches the stall condition. However, in every case, calculations with free wake analysis are in line with the experimental trends, whereas prescribed wake calculations sometimes indicate erroneous trends.

Returning to the two examples given above, but with a rotor load  $C_T/\sigma$  of 0.105, we obtain the following results :

Figure of merit

Rotor	Experi- mental	Calculated	
		prescribed wake	Free wake
Rectangular blades	0.652	0.720	0.710
Tapered blades	0.640	0.730	0.702
Difference	- 0.012	+ 0.010	- 0.008

In order to further improve performance calculation, the weaknesses in the programme must be found by comparing the calculation results with the experimental results for each local point.

### 3.3.2 - Comparison of calculated and experimental induced velocities

Figs. 17 to 19 compare the radial and time patterns of calculated and experimental axial induced velocities. With free wake analysis the correlation between calculation and experiment is qualitatively good. Quantitatively, the axial induced velocities are overestimated by calculation. The excess values calculated for the velocity variations occurring when the tip vortex passes through the measurement plane are obviously due to the lack of a model for the viscous core. It should be noted especially that the velocity peaks are correctly positioned, which proves that the point of intersection between the measurement plane and the tip vortex has been correctly calculated, both in azimuth and in radius, by the method including free wake analysis. The prescribed wake method gives an advance of about  $10^\circ$  in the position of this intersection point.

(EXPERIMENT - CALCULATION COMPARISON  
( $z/R = 0.0677$ )

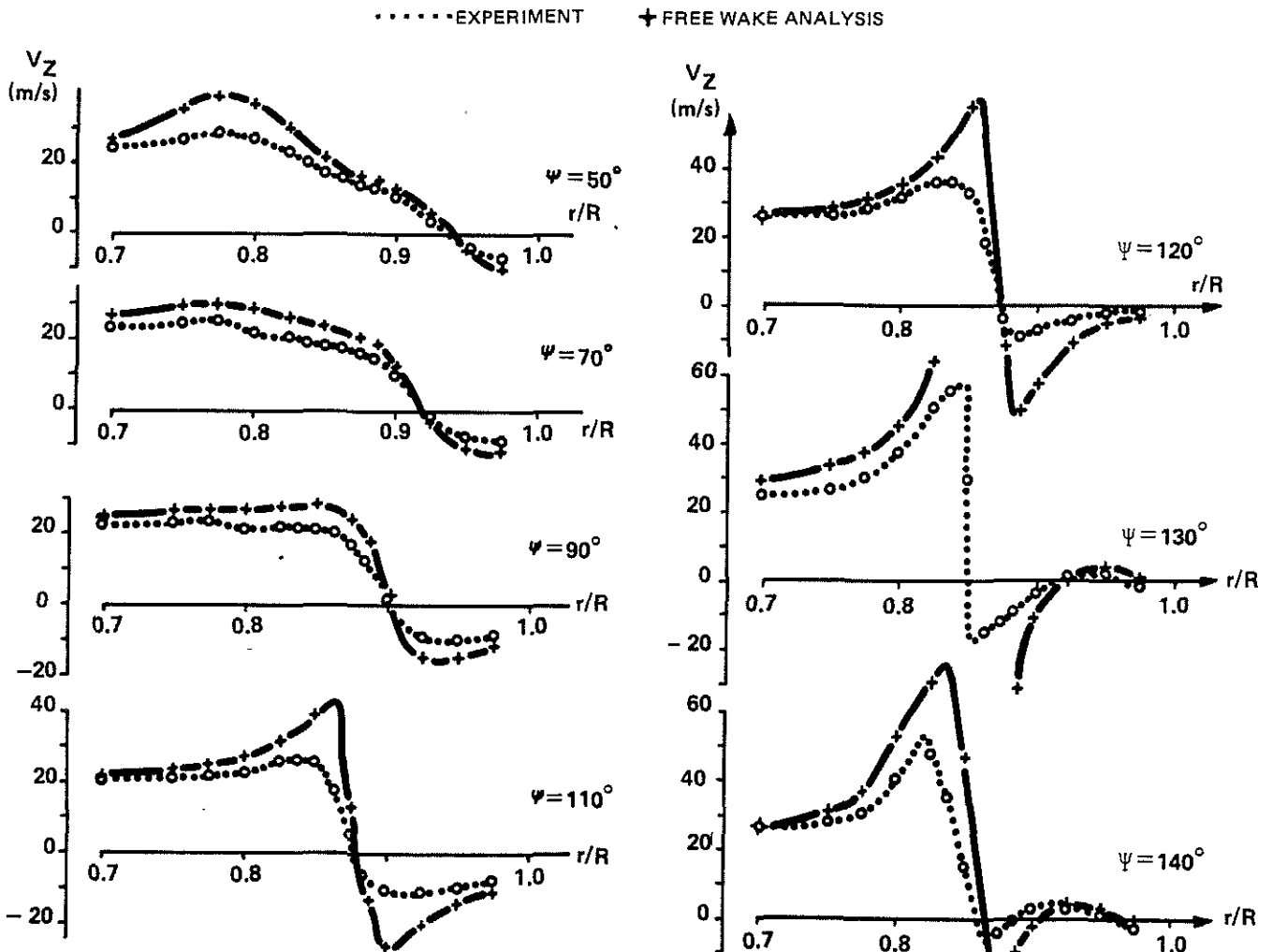


Figure 17

Figure 18

RADIAL DISTRIBUTION OF AXIAL INDUCED VELOCITIES.

(EXPERIMENT - CALCULATION COMPARISON)  
( $z/R = 0.0677$ )

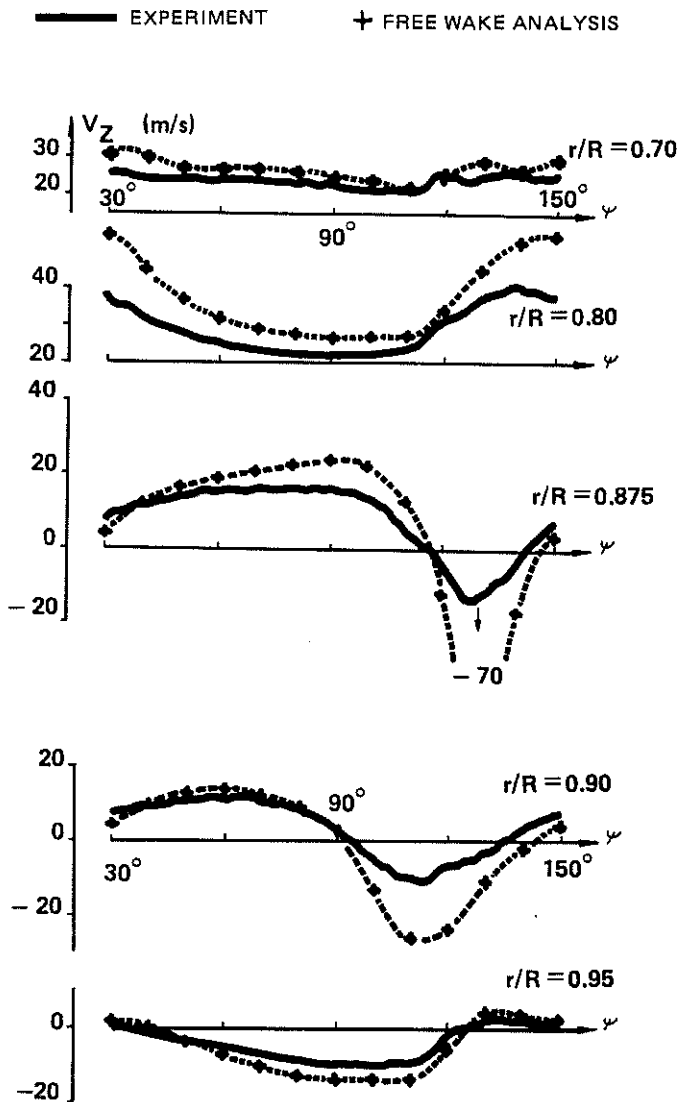


Figure 19 : AZIMUTHAL EVOLUTION OF AXIAL INDUCED VELOCITIES.

Fig. 20 shows the time pattern of the tangential induced velocities for different radii. Here again, with free wake analysis, the correlation between calculation and experimental results is satisfactory. However, it can be noted that although this calculation gives a fair prediction of the tangential velocity peaks observed in the experiments around  $85^\circ$  and  $120^\circ$ , it does not predict the peak that occurred near  $140^\circ$  in azimuth. As we saw in para. 2.3, the first peak is due to the tip vortex passing through the measurement plane. This was thus predicted correctly in the calculation. Analysis of the calculation results leads us to attribute the second peak to circulation around the blade. The third peak is due to a phenomenon which

(EXPERIMENT - CALCULATION COMPARISON)  
( $z/R = 0.0257 - C_T / \sigma = 0.075$ )

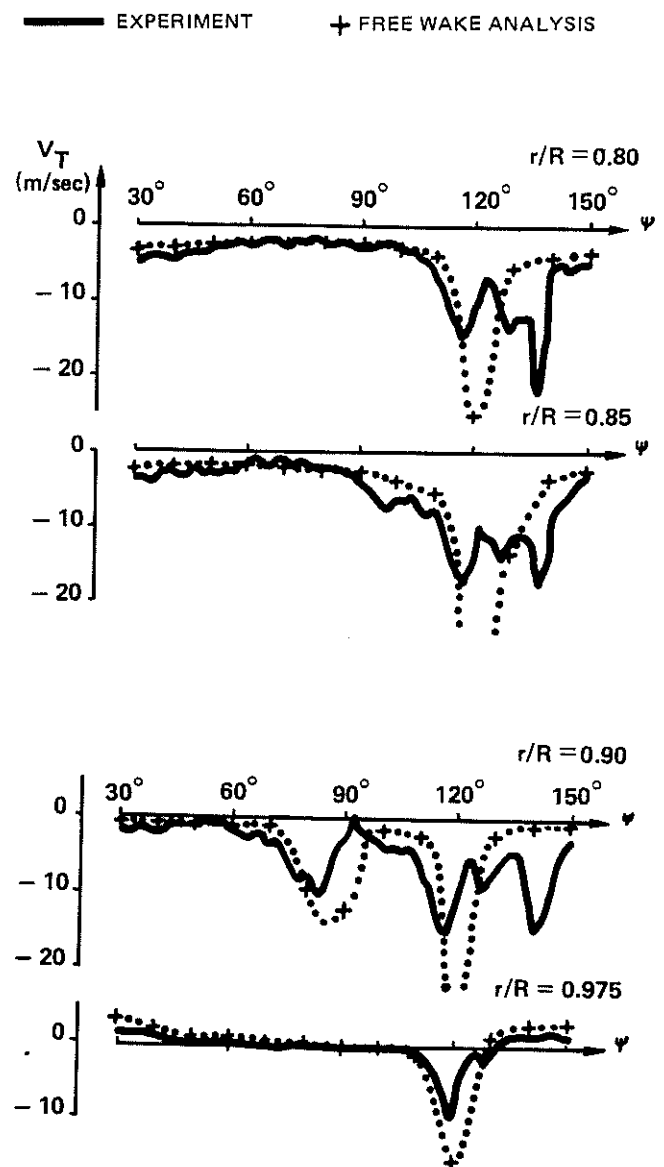


Figure 20 : AZIMUTHAL EVOLUTION OF TANGENTIAL INDUCED VELOCITIES.

is not allowed for in the calculation. In paragraph 2.3 we suggested that it might result from a start of rolling in the vortex sheet ; to verify this hypothesis it would be necessary to schematize this rolling movement in the calculation.

These comparisons all go to show that the passage of the tip vortex through the planes  $z/R = 0.0257$  and  $z/R = 0.0677$  is correctly predicted by free wake analysis.

Fig. 21 shows the calculated and the measured tip vortex paths and confirms that the whole of the vortex path near the rotor disk is accurately predicted by free wake analysis. In the same examples, the prescribed wake analysis gives too high an apparent axial velocity.

EXPERIMENT - CALCULATION COMPARISON

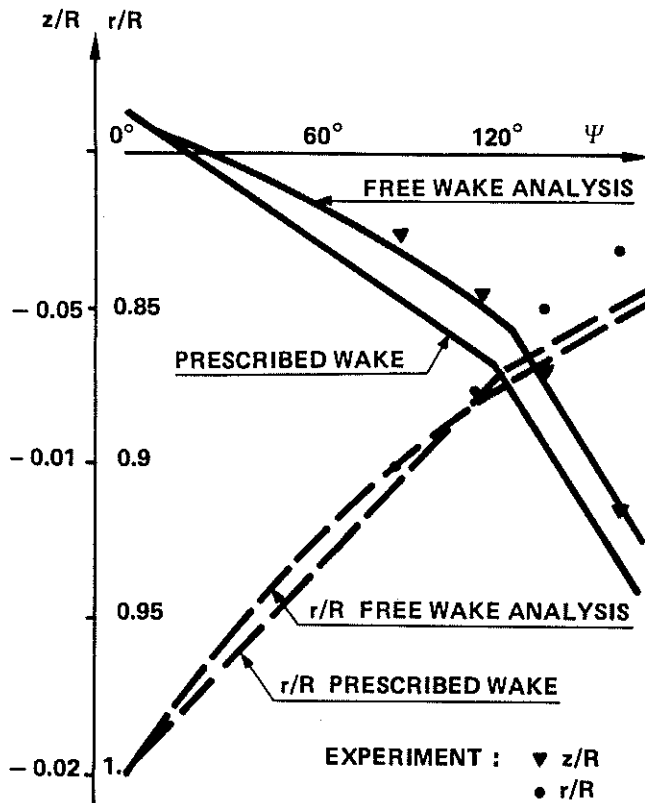


Figure 21 : TIP VORTEX PATH.

#### 4 - CONCLUSION

The experiments conducted by ONERA have shown that laser velocimetrics is a suitable method for studying the wake of a rotor in hover. They have refined our conception of this wake and provided Aerospatiale with the data it requires to improve its performance calculation programme for rotors in hover.

Free wake analysis has greatly improved calculations of performance and the field of induced velocities. There is still more to be done, however, to refine these methods. Various research projects, such as those described in references 4 to 6, have shown the importance of schematizing the viscous vortex core and of the integration method in Biot and Savart's Law for calculating induced velocities. We propose to test various vortex core models, such as those suggested by Rankine (ref. 7) and Scully (ref. 8), and also various laws for tip vortex dissipation (refs 9 and 10). We also plan to compare our method for calculating induced velocities, based on the study by Paget and Elliot (ref. 11), with other methods such as Romberg's (ref. 12) for calculating velocities induced on the blade or that described in reference 13 for calculating the velocity induced by the vortex on itself. Other lines of research may also be considered with a view to improving performance calculation, for example free wake analysis for a larger part of the wake or the technique for simulating

vortex sheets using local vortices, now being developed by ONERA (ref. 14), in order to describe vortex sheet rolling. To give direction to this research, complementary testing is underway at the Institut de Mecanique des Fluides in Marseille, on 2-, 3- and 4-bladed rotors with blades with different plan forms.

#### REFERENCES

- 1 - Experimental and Theoretical Studies on Rotor Blade Tips at O.N.E.R.A.  
J.J. PHILIPPE and J.J. CHATTOT - 6<sup>th</sup> European Rotorcraft and Powered Lift Rotorcraft Forum Bristol September 80
- 2 - A Prescribed wake Lifting Surface Hover Performance Analysis  
J.D. KOCUREK and J.L. TAngLER - 32<sup>nd</sup> Annual National Forum of the American Helicopter Society, May 1976
- 3 - An Analytical and Experimental Investigation of Helicopter Rotor Hover Performance and Wake Geometry Characteristics  
Anton J. LANDGREBE - USA AMRDL TR 71-24 June 1971
- 4 - A Vortex - Wake Analysis of a Single-Bladed Hovering Rotor and a Comparison with Experimental Data  
Robin B. GRAY and George W. BROWN - ACARD CP 111, September 1972
- 5 - Helicopter Hovering Performance Studies  
R.B. GRAY, H.M. Mc MAHON, G. T. BIRD, J.G. PALFERY, S.S. SAMANT and T.P. SHIVANANDA  
Georgia Institute of Technology, Atlanta, October 1976
- 6 - A Lifting-Surface Method for Hover/Climb Airloads  
J. Michael SUMMA and David R. CLARK - 35<sup>th</sup> Annual National Forum of the American Helicopter Society, May 1979
- 7 - Wind Tunnel Simulation of Full Scale Vortices  
J.B. RORKE and R.C. MOFFITT - NASA CR-2180, March 1973
- 8 - Computation of Helicopter Rotor Wake Geometry and its Influence on Rotor Harmonic Airloads  
M.B. SCULLY - MIT A SRL - TR 178-1, March 1971
- 9 - Theory of Lifting Aircrews  
V. Ye BASKIN, L.S. VIL'DGRUBE, Ye S. VOZH-DAYEY, and G.I. MAYKAPAR - NASA TTF-823, 1975
- 10 - Free Wake Analysis of Wind Turbine Aerodynamics  
GOHARD - MIT A SRL - TR 184-8, 1978

- 11 – An Algorithm for Numerical Evaluation of Certain  
CAUCHY Principal Value Integrals  
PAGET and ELLIOT - Numerish Mathematik, 1972
- 12 – Numerical Methods  
R.W. HORNBECK - Quantum Publishing, Inc. New  
York, N.Y., 1975
- 13 – The Structure and Dynamics of Vortex Filaments  
S.E. WINDNALL - Annual Review of Fluid Mechanics  
Vol. 7, 1975
- 14 – Numerical Calculation of 3D Unsteady Flows with  
Vortex Sheets  
C. REHBACH - AIAA Paper n° 78-111